Journal of Membrane Science 566 (2018) 307–316

Contents lists available at ScienceDirect

Journal of Membrane Science

journal homepage: www.elsevier.com/locate/memsci

Effect of fixed charge group concentration on salt permeability and diffusion coefficients in ion exchange membranes

Jovan Kamcev[a], Cara M. Doherty[b], Kian P. Lopez[a], Anita J. Hill[b], Donald R. Paul[a], Benny D. Freeman[a,*]

[a] McKetta Department of Chemical Engineering, Center for Energy and Environmental Resources, and Texas Materials Institute, The University of Texas at Austin, 10100 Burnet Road Building 133 (CEER), Austin, TX 78758, USA
[b] CSIRO Manufacturing, Private Bag 10, Clayton South MDC, Clayton, VIC 3169, Australia

ARTICLE INFO

Keywords:
Ion exchange membrane
Salt permeability coefficient
Salt diffusion coefficient
Positron annihilation lifetime spectroscopy

ABSTRACT

This report presents a systematic investigation of the influence of fixed charge group concentration on salt diffusion coefficients in ion exchange membranes. Cross-linked cation and anion exchange membranes (CEMs and AEMs) having different fixed charge group concentrations and similar water content were synthesized via a one-step free radical copolymerization reaction. Concentration gradient-driven ion transport through the membranes was probed by measuring salt permeability coefficients as a function of salt concentration in the upstream solution. For all membranes, salt permeability coefficients increased by approximately one order of magnitude as external solution salt concentration increased from 0.01 to 1 M, predominantly due to similar increases in salt partition coefficients. On average, salt permeability coefficients for both series of membranes decreased with increasing fixed charge group concentration to nearly the same extent. Apparent salt diffusion coefficients, which were extracted from salt permeability and salt partition coefficients via the solution-diffusion model, changed to a greater extent for the AEMs than those for the CEMs despite similar changes in membrane fixed charge group concentration. The relative changes in apparent salt diffusion coefficients between AEMs and CEMs were attributed to differences in free volume of the membranes. This hypothesis was supported by positron annihilation lifetime spectroscopy measurements, which demonstrated variation in ortho-positronium lifetime values (a measure of free volume element size) for these membranes that correlated with variations in apparent salt diffusion coefficients.

1. Introduction and background

Rapidly increasing demands for clean water have fueled an intense search for inexpensive and energy efficient technologies to address this need [1–3]. In particular, membrane-based technologies have attracted significant interest owing to their energy efficiency, small footprint, and operational simplicity [4–8]. Reverse osmosis (RO) is the most widely implemented seawater desalination process [7], but other technologies such as electrodialysis [9,10], forward osmosis [11,12], and membrane assisted capacitive deionization [13,14], are rapidly gaining traction in this space. Membranes, which are typically made from polymers, play a central role in these technologies because of their ability to selectively transport water and ions [5,15]. The optimal membrane properties in terms of water/ion permeability and selectivity can vary widely depending on the application. For example, RO membranes must effectively permeate water and reject salt [7], while electrodialysis membranes must selectively permeate ions and reject water [10]. Currently, no general guidelines exist for rational design of high performance membranes having a particular set of water and ion transport properties. Such an endeavor requires fundamental understanding of the influence of polymer structure on ion and water transport through membranes.

The membranes used for applications requiring separation of small solutes of comparable size (e.g., water and ions) are typically dense (i.e., nonporous) [5]. Small solute transport in dense membranes is driven by a chemical potential gradient, or electrochemical potential gradient in the case of ions, and described by the solution-diffusion mechanism [15–17]. According to this framework, solutes first partition into the membrane at the high chemical (or electrochemical) potential side of a membrane. Solute partitioning between a membrane and solution is often governed by the relative magnitude of interactions between the solute and the two phases. The solutes then diffuse across the membrane down a chemical (or electrochemical) potential gradient,

* Corresponding author.
E-mail address: freeman@che.utexas.edu (B.D. Freeman).

https://doi.org/10.1016/j.memsci.2018.08.053
Received 20 June 2018; Received in revised form 15 August 2018; Accepted 25 August 2018
Available online 29 August 2018
0376-7388/

and subsequently partition back into the solution at the low chemical (or electrochemical) potential side. Fundamental understanding of the phenomena governing solute partitioning and diffusion in a membrane would facilitate design of high performance membranes with specifically tailored transport properties.

Recently, ion exchange membranes (IEMs) have attracted significant interest for membrane-based technologies owing to their chemical stability and desirable ion and water transport properties [15,18–20]. IEMs are made from polymers having ionizable functional groups covalently bound to their backbone [21]. Such functional groups can be appended to a broad range of polymer chemistries, giving rise to a rich diversity of polymers that can be used to form IEMs [18,21]. Ionizable functional groups covalently bound to a polymer backbone profoundly influence ion/water partitioning and transport through such membranes [15,20–32]. For example, highly charged IEMs typically sorb a significantly greater number of counter-ions (i.e., ions with opposite charge to that of fixed charges) than co-ions (i.e., ions with similar charge to that of fixed charges) since counter-ions must electrically balance the fixed charge groups, which are typically present at high concentrations [22,23,25,33]. Consequently, such membranes exhibit low co-ion permeability and high counter-ion permeability. The former property is useful for applications in which co-ion transport must be hindered (e.g., reverse osmosis [34]), whereas the latter property is useful for applications in which fast, selective counter-ion transport is required (e.g., electrodialysis [10], batteries [35–37]). A recent extensive review on IEMs nicely summarizes the current state of understanding of ion transport and selectivity in such materials and points out some important missing knowledge gaps [38].

IEMs have been the subject of academic interest for a long time [21,39], but a complete fundamental understanding of the influence of fixed charge groups on ion transport in such materials is still missing. One roadblock impeding production of such knowledge is the difficulty encountered in systematically changing one membrane property while keeping all other properties constant. For example, changing the fixed charge group concentration of a membrane often simultaneously changes its water content, making it difficult to attribute observed changes in transport properties to one variable over the other [27,40]. Recently, we reported the synthesis of a series of cross-linked ion exchange membranes having different fixed charge group concentrations but similar water content via a one-step cross-linking polymerization reaction [25]. The membrane fixed charge group concentration was varied by controlling the amount of charged monomer in the prepolymer solution, while the membrane water content was controlled by varying the effective cross-link density [25]. Our previous study investigated the influence of fixed charge group concentration on equilibrium ion partitioning between an ion exchange membrane and aqueous salt solution. The present study builds upon this work and focuses on the influence of fixed charge group concentration on salt diffusion and permeability coefficients in IEMs when ion transport is driven by a concentration gradient. Improved fundamental understanding of ion transport in IEMs driven by a concentration gradient could facilitate rational design of high performance membranes for processes such as reverse osmosis, forward osmosis, and Donnan dialysis, among others.

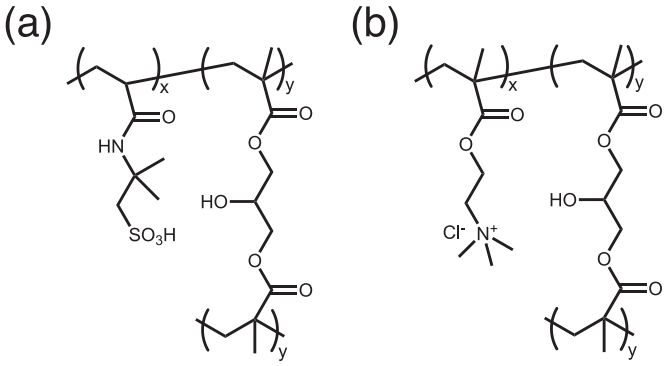

Fig. 1. Chemical structures of the polymers used in this study: (a) cation exchange membranes and (b) anion exchange membranes.

2. Experimental

2.1. Membranes

The membranes used in this study were synthesized via a free radical copolymerization reaction [25,41,42]. In a typical experiment, a charged monomer, cross-linker, and radical forming initiator were dissolved in a mutual solvent and polymerized between two glass plates separated by metal spacers to afford free-standing ion exchange membranes. The synthesis procedure is described in detail elsewhere [25]. The chemical structures and relevant properties of the membranes, including water volume fraction, ϕ_w, and fixed charge group concentration, C_A^m, are presented in Fig. 1 and Table 1, respectively. Prior to all measurements, the membranes were equilibrated with ultrapure deionized (DI) water. The equilibration procedure involved soaking the membranes in DI water for at least 24 h and periodically replacing the DI water. Ultrapure DI water (18.2 MΩ-cm electrical resistivity and less than 5.4 ppb TOC) was generated by a Millipore RiOS and A10 water purification system (Billerica, MA).

2.2. Salt permeability coefficients

Salt permeability coefficients were measured using custom jacketed glass diffusion cells (PermeGear Side-Bi-Side Custom Diffusion Cell, Hellertown, Pennsylvania) according to a previously reported

Table 1
Relevant properties of the membranes used in this study [25].

Sample[a]	Theoretical IEC [meq/g]	Exp. IEC [meq/g]	Gel fraction	ϕ_w [L (water)/L (swollen membrane)]	C_A^m [mols /L (swollen membrane)]
CA200	2.00 (H^+)	1.99 ± 0.052 (H^+)	0.989 ± 0.005	0.568 ± 0.005	1.13 ± 0.01
CA238	2.38 (H^+)	2.43 ± 0.053 (H^+)	0.990 ± 0.001	0.570 ± 0.010	1.38 ± 0.02
CA267	2.67 (H^+)	2.68 ± 0.025 (H^+)	0.983 ± 0.005	0.571 ± 0.003	1.52 ± 0.01
AA200	2.00 (Cl^-)	2.01 ± 0.052 (Cl^-)	0.960 ± 0.011	0.498 ± 0.009	1.27 ± 0.03
AA238	2.38 (Cl^-)	2.25 ± 0.064 (Cl^-)	0.976 ± 0.008	0.500 ± 0.003	1.53 ± 0.04
AA267	2.67 (Cl^-)	2.48 ± 0.039 (Cl^-)	0.939 ± 0.004	0.497 ± 0.007	1.70 ± 0.02

[a] The samples are named as CAXXX and AAXXX for cation and anion exchange membranes, respectively, where "XXX" denotes 100 times the theoretical IEC value.

procedure [43]. A DI water-equilibrated membrane sample was clamped between the two glass diffusion cells. The downstream chamber was filled with 35 mL of DI water, and a conductivity probe (WTW LR 325/01, Weilheim, Germany) was inserted into the chamber. The downstream chamber was sealed with Parafilm to prevent solution evaporation during the measurement. The upstream chamber was filled with 35 mL of aqueous NaCl solution. The solutions were stirred with magnetic stir bars during the experiment. The temperature of the solutions in the chambers was maintained at 25 °C via a circulator bath (Thermo NESLAB RTE 10, Waltham, Massachusetts), and the apparatus was exposed to the atmosphere. Changes in solution ionic conductivity over time in the downstream chamber due to NaCl permeation across the membrane were recorded using aWTW inoLab Cond 730 Conductivity Meter (Weilheim, Germany). Ionic conductivity in the downstream solution was converted to NaCl concentration via a calibration curve.

Following completion of the experiment, the cell was quickly disassembled, and the membrane thickness was measured using a micrometer (Mitotuyo Series 293, Aurora, IL). The salt permeability coefficient, $<P_s>$, was determined by fitting the experimental data to [43,44]:

$$\ln\left[1-\frac{2(C_s^s)_{\ell}[t]}{(C_s^s)_0[0]}\right] = -\left(\frac{2A_m < P_s >}{V\ell}\right)t \quad (1)$$

where $(C_s^s)_{\ell}[t]$ is the molar NaCl concentration in the downstream solution at time t, $(C_s^s)_0[0]$ is the initial NaCl concentration in the upstream chamber, A_m is the geometric area available for mass transfer (1.77 cm^2), V is the volume of the upstream and downstream solutions (35 mL), and ℓ is the membrane thickness.

Dissolution and subsequent speciation of ambient CO_2 into the aqueous solutions during the experiment can influence salt permeability measurements, especially when studying anion exchange membranes and when the salt concentration in the upstream chamber is low (e.g., < 0.1 M) [43]. Ambient CO_2 dissolves in aqueous solutions to form H_2CO_3, which then speciates into H^+, HCO_3^-, and CO_3^{2-} ions [43,45]. During the permeability measurements, these ions replace the counter-ions initially present in the membrane, thereby interfering with the downstream conductivity measurements. This issue can be mitigated by bubbling ultra-high purity N_2 gas into the aqueous solutions during the permeability measurements. This modification to the experimental procedure is described in detail elsewhere and was fully adopted in the present study [43].

2.3. Positron annihilation lifetime spectroscopy

The average free volume element size and distribution of the membranes were determined in both the wet and dry states using Positron Annihilation Lifetime Spectroscopy (PALS). The membranes were initially dried at 50 °C in a vacuum oven overnight before being measured in a dry nitrogen atmosphere. The membranes were cut and stacked to 4 mm with a Mylar sealed ^{22}NaCl positron source placed in the middle of the sample. The samples were measured using an EG&G Ortec fast-fast spectrometer set to coincidence with a resolution of 240 ps. The samples were measured for 5×10^6 integrated counts (approximately 12 h) and fitted to three components and a source correction (1.622 ns, 3.41%) using the LT-v9 software [46]. The first component, attributed to para-positronium formation (*p*-Ps) was fixed to 0.125 ns. The second component was attributed to free annihilation (~ 0.4 ns) and the third component was attributed to ortho-positronium (*o*-Ps) annihilation. The *o*-Ps lifetime (τ_3) was used to calculate the average free volume element size of the membranes using the Tao-Eldrup equation [47,48]. After the dry measurements, the membranes were immersed in water overnight and measured in a sealed sample holder to prevent evaporation.

3. Results and discussion

3.1. Membrane water content and fixed charge group concentration

Evaluating the influence of fixed charge group concentration on salt diffusion in water-swollen ion exchange membranes requires systematic variation of membrane fixed charge group concentration independently from other membrane properties that influence salt diffusion in such materials (e.g., chemical structure and membrane water content). In particular, membrane water content, typically quantified by the volume fraction of water in a membrane, significantly influences salt diffusion in IEMs since salt diffusion occurs within the aqueous regions of a membrane [4,44,49,50]. In general, increasing membrane water content increases salt diffusion coefficients and vice versa [50]. In an early study, Yasuda et al. reported a strong inverse correlation between salt diffusion coefficients and membrane water volume fraction in a series of uncharged hydrogels [44]. The authors explained this behavior within the framework of free volume theory by assuming that the free volume of a hydrated membrane is linearly proportional to the volume fraction of water that the membrane absorbed [44]. Yasuda's model has found relatively widespread success in describing salt diffusion in water swollen membranes [40,50]. Consequently, maintaining constant membrane water content (i.e., membrane water volume fraction) while systematically varying the membrane fixed charge group concentration is critical to isolate the effect of fixed charge group concentration on salt diffusion coefficients in IEMs.

The volume fraction of water in a cross-linked membrane depends largely on the density of elastically effective cross-links (i.e., cross-links that contribute to the mechanical properties of a polymer network) [50]. Addition of solvent during a cross-linking polymerization reaction often leads to formation of elastically ineffective cross-links (e.g., cross-link loops), thereby providing an avenue for controlling membrane water content. For example, increasing the amount of solvent in a prepolymerization mixture typically increases the probability of forming elastically ineffective cross-links and subsequently increases membrane water content [50–52]. In the present study, this strategy was used to control the volume fraction of water in the membranes independently from fixed charge group concentration.

The dependence of membrane water volume fraction on NaCl concentration in the external solution for the materials considered in this study is presented in Fig. 2a. For all membranes, water volume fraction values were relatively constant at low NaCl concentrations (< 0.1 M) and decreased at higher NaCl concentrations (> 0.1 M) due to osmotic deswelling, a phenomenon generally observed for such materials [53]. Within the experimental uncertainties, water volume fraction values for all CEMs and all AEMs were essentially the same over the entire NaCl concentration range explored.

Membrane fixed charge group concentration values, expressed in units of mols of fixed charge groups per L of swollen membrane (volume includes contributions from ions, water, and polymer chains), are presented in Fig. 2b as a function of theoretical IEC. Membrane fixed charge group concentrations were taken to be equivalent to membrane counter-ion concentrations for membranes equilibrated with 0.01 M NaCl solutions, since membrane co-ion concentrations are orders of magnitude lower than counter-ion concentrations at these conditions [25]. That is, nearly all of the counter-ions in the membranes are electrically balancing the fixed charge groups. As anticipated, fixed charge group concentrations for the CEMs and AEMs increased with increasing theoretical IEC owing to increased amounts of ion containing monomer incorporated in the polymer network. For both series of membranes, fixed charge group concentrations increased by approximately 21% and 34% as theoretical IEC values increased from 2.00 to 2.38 and 2.67, respectively. The results presented in Fig. 2 confirm the successful synthesis of IEMs having different fixed charge group concentrations and similar water content.

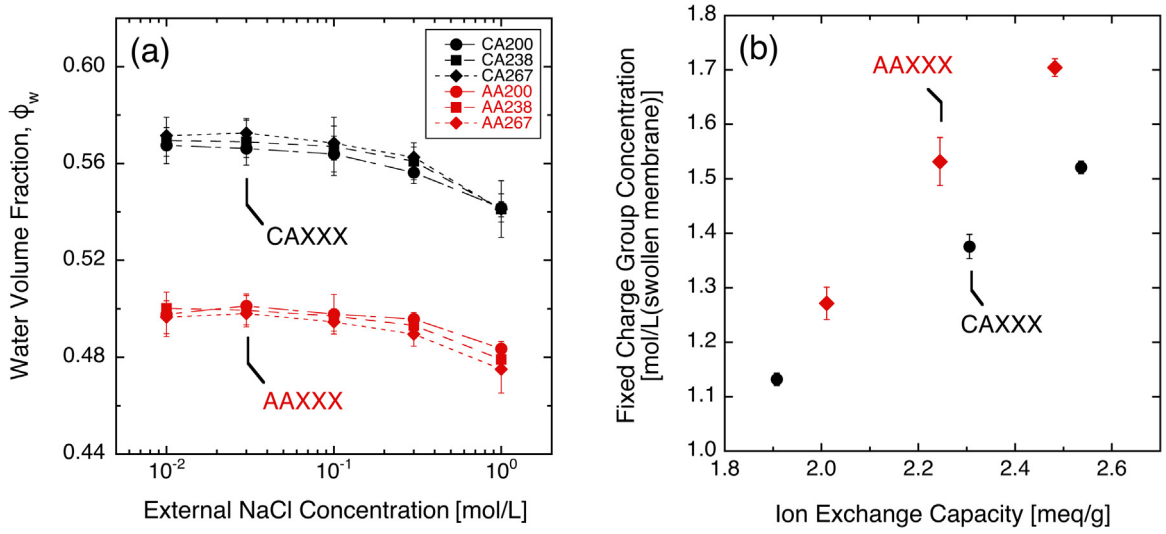

Fig. 2. (a) Volume fraction of water in the membranes as a function of NaCl concentration in the external solution [25]. (b) Fixed charge group concentration in the membranes as a function of theoretical ion exchange capacity. Uncertainties represent the standard deviation of measurements on at least 6 different samples.

3.2. NaCl permeability and partition coefficients

Concentration gradient driven ion transport in membranes is typically quantified by the salt permeability coefficient, which is defined as the steady state salt flux through a membrane normalized by membrane thickness and salt concentration difference between the upstream and downstream solutions [17,26,44]. According to the solution-diffusion model, salt permeability coefficients, $<P_s>$, are related to salt partition (i.e., sorption) coefficients, K_s, and apparent salt diffusion coefficients, $<\bar{D}_s^{m*}>$, via $<P_s> = K_s < \bar{D}_s^{m*}>$ [17]. Salt partition coefficients are defined as $K_s = C_s^m/C_s^s$, where C_s^m is the mobile salt concentration in the membrane and C_s^s is the salt concentration in the contiguous (i.e., external) solution. For 1:1 electrolytes, the mobile salt concentration in an ion exchange membrane is equivalent to the co-ion concentration.

NaCl permeability coefficients for the membranes in this study were measured as a function of upstream NaCl concentration, ranging from 0.01 to 1 M, according to the procedure described in the Experimental section, and the results are presented in Fig. 3. For all membranes, NaCl permeability coefficients increased by approximately one order of magnitude as upstream NaCl concentration increased from 0.01 to 1 M. The strong salt concentration dependence of salt permeability coefficients has been observed in other highly charged ion exchange membranes, and it is attributed predominantly to the salt concentration dependence of salt partition coefficients in such materials, as demonstrated below. For comparison, salt permeability coefficients of uncharged membranes are often relatively constant over similar salt concentration ranges [52].

For both series of IEMs, increasing the fixed charge group concentration while maintaining constant water content decreased NaCl permeability coefficients to a similar extent. For example, NaCl permeability coefficients for CA267 and AA267 were approximately 37% and 35% lower on average than those for CA200 and AA200, respectively. This result is intuitive within the framework of the solution-diffusion model since increasing the fixed charge group concentration of a membrane enhances electrostatic (i.e., Donnan) exclusion of ions from the membrane, decreasing salt partition coefficients and, consequently, decreasing salt permeability coefficients. However, previous studies on ion exchange membranes made from linear polymers in

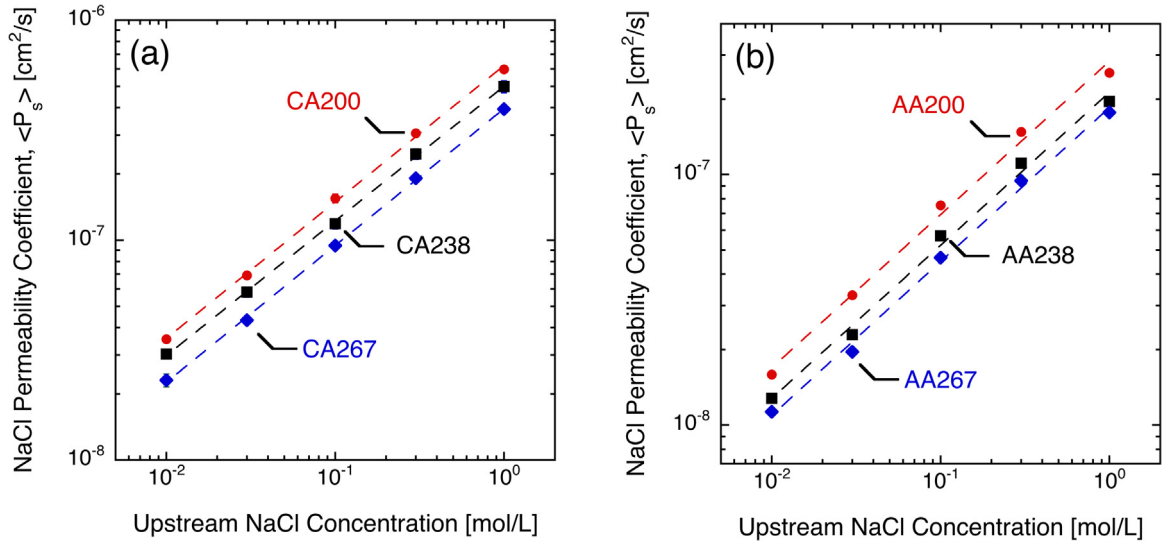

Fig. 3. Salt permeability coefficients as a function of upstream NaCl concentration for: (a) cation exchange membranes CA200, CA238, and CA267 and (b) anion exchange membranes AA200, AA238, and AA267. The dashed lines were drawn to guide the eye. Uncertainties represent the standard deviation of measurements on at least 6 different samples.

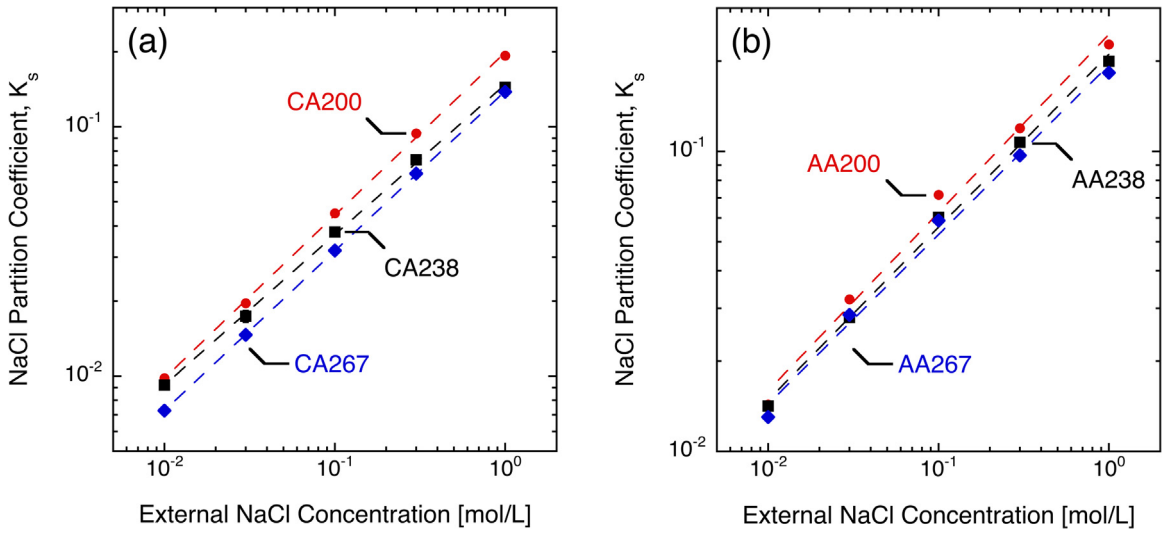

Fig. 4. NaCl partition coefficients as a function of external solution NaCl concentration for: (a) cation exchange membranes CA200, CA238, and CA267, and (b) anion exchange membranes AA200, AA238, and AA267 [25]. The dashed lines were drawn to guide the eye. Uncertainties represent the standard deviation of measurements on at least 6 different samples.

which the membrane IEC values were systematically varied reported the opposite behavior, i.e., NaCl permeability coefficients increased with increasing IEC [27,40]. This counter-intuitive result can be explained by considering changes in membrane water content with changes in IEC. Increasing the IEC of membranes made from linear polymers typically increases membrane water content due to increased hydrophilicity of the polymer chains, which essentially dilutes the concentration of fixed charge groups in the swollen membrane, thereby enhancing ion sorption in the membranes [27,40]. Indeed, IEC is not a particularly informative metric for quantifying the fixed charge group concentration of a swollen membrane since IEC values are based on the dry polymer. Moreover, as mentioned earlier, increased membrane water content typically increases salt diffusion coefficients, which also contributes to increased salt permeability coefficients. These results underscore the necessity of maintaining constant membrane water content if one wishes to suppress salt permeability coefficients in IEMs by increasing the membrane fixed charge group concentration.

NaCl partition coefficients for the membranes in this study were calculated from previously reported equilibrium ion sorption results and are presented in Fig. 4 as a function of NaCl concentration in the external solution [25]. For all membranes, NaCl partition coefficients increased by approximately one order of magnitude as external solution NaCl concentration increased from 0.01 to 1 M. The increase in NaCl partition coefficients with increasing external solution NaCl concentration is caused by weakening of the Donnan potential at the membrane/solution interface, as discussed in considerable detail elsewhere [25].

For both series of IEMs, increasing the fixed charge group concentration at constant water content decreased NaCl partition coefficients, presumably due to enhanced Donnan exclusion. However, the decrease in NaCl partition coefficients for the CEMs was more pronounced than that for the AEMs, despite similar changes in fixed charge group concentrations. For example, NaCl partition coefficients for CA267 were approximately 28% lower on average than those for CA200, while NaCl partition coefficients for AA267 were approximately 15% lower on average than those for AA200. This result was previously rationalized within the framework of a model based on Donnan theory combined with Manning's counter-ion condensation theory for polyelectrolyte solutions [25,54]. Briefly, the weaker influence of fixed charge group concentration on NaCl partitioning in the AEMs was attributed to condensation of counter-ions on the polymer backbone. Counter-ion condensation in the AEMs weakened the Donnan potential at the membrane/solution interface since condensed counter-ions are effectively neutralized by the fixed charge groups and presumably do not contribute to the Donnan potential. After accounting for counter-ion condensation, the “effective” fixed charge group concentrations for all AEMs were quite similar, resulting in little change in NaCl partition coefficients for these materials. In contrast, counter-ion condensation did not occur in the CEMs and all counter-ions contributed to the Donnan potential, so the “effective” fixed charge group concentration increased to a greater extent with increasing IEC relative to that of the AEMs. Thus, the co-ion sorption decrease with increasing fixed charge group concentration in the CEMs was stronger than that for the AEMs. The interested reader is referred to our previous report for a more detailed explanation of this phenomenon [25].

3.3. Apparent salt diffusion coefficients

Apparent salt diffusion coefficients, $<\bar{D}_s^{m*}>$, were calculated from experimentally measured salt permeability and salt partition coefficients via the solution-diffusion model. These values are “apparent” because they are not corrected for frame of reference (i.e., convection) and thermodynamic non-ideal effects [24]. Previously, it was demonstrated that such effects act in opposite directions and essentially cancel out for ion exchange membranes that have properties similar to those considered here, so these effects are ignored in the discussion below [24]. The final results are presented in Fig. 5. Within experimental uncertainties, apparent salt diffusion coefficients were relatively constant over the external solution salt concentration range explored in this study. These results confirm the hypothesis that the salt concentration dependence of salt permeability coefficients for these materials stems from the salt concentration dependence of salt partition coefficients (cf. Fig. 4) rather than apparent salt diffusion coefficients, which agrees with previous reports on other highly charged IEMs [26]. For both series of IEMs, apparent salt diffusion coefficients decreased on average with increasing fixed charge group concentration. However, despite similar increases in fixed charge group concentrations, apparent salt diffusion coefficients for the AEMs decreased more, on average, than those for the CEMs. For example, apparent salt diffusion coefficients for CA267 were approximately 12% lower, on average, than those for

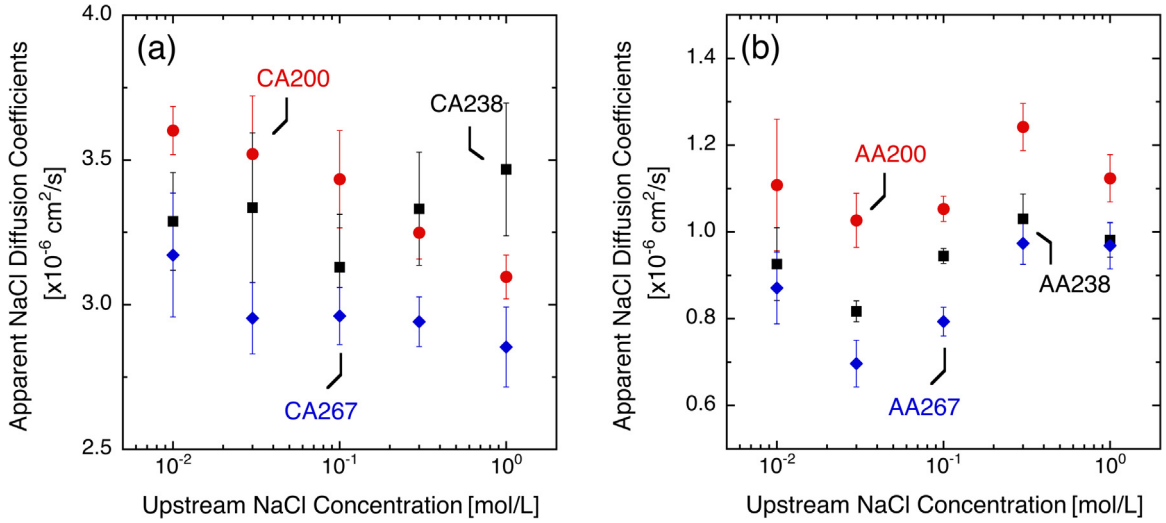

Fig. 5. Apparent salt diffusion coefficients as a function of upstream solution NaCl concentration for: (a) cation exchange membranes CA200, CA238, and CA267 and (b) anion exchange membranes AA200, AA238, and AA267. Uncertainties were calculated via propagation of errors from the uncertainties of salt permeability and partition coefficients measurements.

CA200, while apparent salt diffusion coefficients for AA267 were approximately 23% lower, on average, than those for AA200.

Previously, we hypothesized that salt diffusion coefficients in relatively highly swollen, highly charged IEMs are affected by a tortuosity effect as well as electrostatic interactions between the fixed charge groups and mobile ions [26]. The tortuosity effect was modeled via the Mackie and Meares model [55], and electrostatic effects were modeled via Manning's counter-ion condensation theory [56]. The model provided reasonably good predictions for salt permeability coefficients in a series of commercial IEMs with no adjustable parameters. In the Mackie and Meares model, ion diffusion in homogeneous ion exchange membranes is presumed to occur within interconnected aqueous regions in the membrane [55]. Ion diffusion coefficients in the membrane are assumed to be similar to those in aqueous salt solutions. However, the polymer chains are effectively stationary, at least over timescales relevant to ion diffusion in a membrane, and act as impenetrable obstructions that increase the total distance ions must travel to cross the membrane relative to an aqueous solution of equivalent thickness, thereby giving rise to a tortuosity effect. The model neglects specific interactions between ions and polymer chains. As a consequence of the tortuosity effect, experimentally measured salt diffusion coefficients in membranes are lower than values observed in aqueous solutions [55]. Mackie and Meares used an approach based on a simple cubic lattice to derive an expression for the tortuosity factor. Their final result is [55]:

$$\frac{D_i^m}{D_i^s} = \frac{\phi_w}{2-\phi_w} \tag{2}$$

where D_i^m is the ion diffusion coefficient in a membrane, D_i^s is the ion diffusion coefficient in aqueous solution, and ϕ_w is the membrane water volume fraction. According to this model, D_i^m depends only on the volume fraction of water in a membrane. Since the water volume fractions for the CEMs as well as those for the AEMs are essentially the same, this model cannot explain the results observed in Fig. 5, i.e., salt diffusion coefficients decreased on average with increasing fixed charge group concentration.

Manning's counter-ion condensation theory for ion diffusion in polyelectrolyte solutions was formulated on the assumption that fixed charge groups on a charged polymer create a locally inhomogeneous electric field in the vicinity of the polymer chains that influences ion diffusion [56]. Manning described the inhomogeneous electric fields using a Debye-Hückel approximation and derived predictive expressions relating ion diffusion coefficients in such systems to ion diffusion coefficients in aqueous solutions in the absence of polyelectrolyte chains. Manning's model requires two parameters, the non-dimensional linear charge density, ξ, which can be calculated from the average distance between fixed charge groups and dielectric constant of a hydrated membrane, and X, which is the ratio of the fixed charge group concentration to the mobile salt concentration of a membrane (i.e., $X = C_A^m/C_s^m$). Manning's model was applied to the membranes in this study (see Supplementary information section for details and calculations), but the model also failed to explain the observed decrease in salt diffusion coefficients with increasing fixed charge group concentration, suggesting that electrostatic effects are not the cause for this behavior.

3.4. Positron annihilation lifetime spectroscopy

To experimentally probe the influence of polymer structure on salt diffusion coefficients, dry and hydrated polymer films were characterized via positron annihilation lifetime spectroscopy (PALS). PALS is a useful technique for quantifying free volume in polymers by measuring the lifetime and intensity of o-positronium (*o*-Ps) as they form and annihilate within polymer samples exposed to a sealed positron source (often ^{22}Na) [57–60]. This technique has been widely used to correlate polymer free volume and solute transport in polymer membranes for both gas and liquid separations [40,50,57,61–65]. In particular, the lifetime (τ_3) and intensity (I_3) of *o*-Ps has been correlated with the average size and concentration (i.e., density), respectively, of free volume elements in polymers [65]. Assuming that free volume elements in a polymer can be modeled as a distribution of spherical cavities, τ_3 can be related to the average radius of a spherical free volume element, r, via [47,48,65]:

$$\tau_3 = \frac{1}{2}\left(1-\frac{r}{r+\Delta r} + \frac{1}{2\pi}\sin\left[2\pi\frac{r}{r+\Delta r}\right]\right)^{-1} \tag{3}$$

where Δr is the empirical electron layer thickness, which is calculated to be 1.66 Å [65]. Consequently, the average volume of a spherical free volume element is given by:

$$V_{FVE} = \frac{4}{3}\pi r^3 \tag{4}$$

Upon exposure to positrons, *o*-Ps forms and annihilates in the low electron density regions of the polymer (i.e., the free volume regions). However, this formation and annihilation process can be obfuscated by the chemical nature of a polymer. For example, previous studies have demonstrated that the presence of electron withdrawing groups (e.g.,

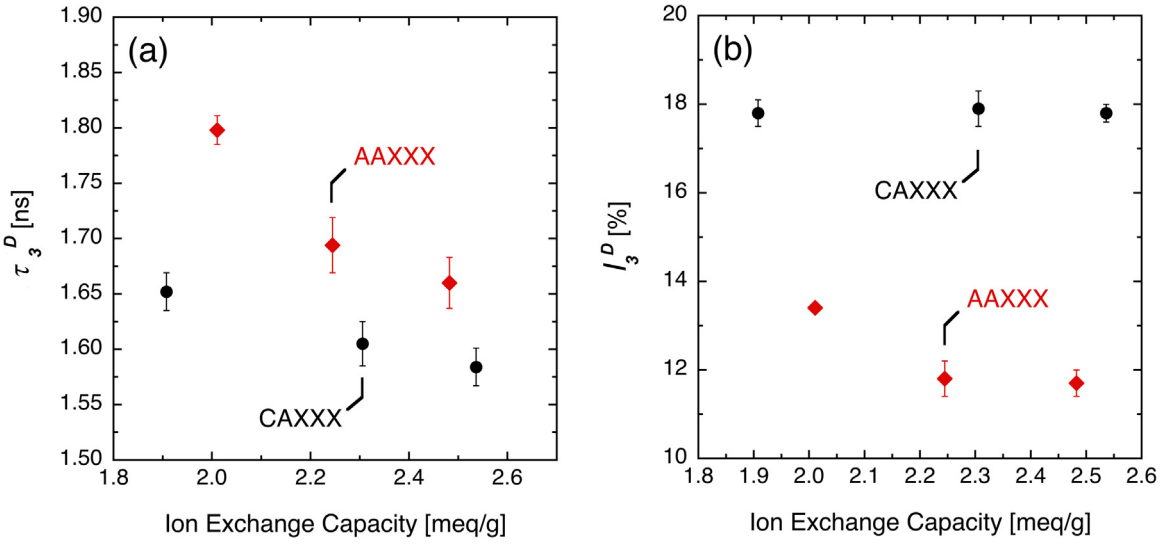

Fig. 6. *o*-Ps lifetime (a) and intensity (b) of dry membrane samples as a function of ion exchange capacity. Reported uncertainties are the population standard deviation of measurements on at least 5 sets of data with 1×10^6 integrated counts for each set.

Table 2
Positron annihilation lifetime spectroscopy results for dry membranes.

Membrane	τ_3^D [ns]	I_3^D [%]	r^D [nm]	V_{FVE}^D [Å^3]
CA200	1.652 ± 0.017	17.8 ± 0.3	0.502 ± 0.004	66.3 ± 1.4
CA238	1.605 ± 0.020	17.9 ± 0.4	0.492 ± 0.004	62.3 ± 1.7
CA267	1.584 ± 0.017	17.8 ± 0.2	0.487 ± 0.004	60.6 ± 1.4
AA200	1.798 ± 0.013	13.4 ± 0.1	0.532 ± 0.003	78.9 ± 1.2
AA238	1.694 ± 0.025	11.8 ± 0.4	0.511 ± 0.005	69.8 ± 2.2
AA267	1.660 ± 0.023	11.7 ± 0.3	0.505 ± 0.005	67.0 ± 1.9

sulfonates, halides) on a polymer backbone could inhibit formation of *o*-Ps [40,60,62,65–67]. This inhibition is an important issue because ion containing polymers often contain such chemical functionalities. If such effects were to take place, the *o*-Ps intensity (I_3) would not be an accurate measure of the density of free volume elements. Considering the presence of electron withdrawing groups within the ion exchange membranes used in this study, and previous studies showing the likelihood of inhibition occurring [39,61], we have herein limited our interpretation of I_3. Further studies would be needed to confirm that there are no effects from inhibition for these materials. The *o*-Ps lifetime is unaffected by inhibition, making it possible to extract information regarding the average size of free volume elements in such materials [40,65].

Although *o*-Ps lifetime and intensity values for hydrated membrane samples are more relevant when investigating ion transport in such materials, it is also instructive to probe the dependence of these parameters on fixed charge group concentration in dry membranes, as well as changes in these values upon hydration. *o*-Ps lifetime and intensity values for the dry membranes, τ_3^D and I_3^D, respectively, are presented in Fig. 6 as a function of membrane IEC. For convenience, the PALS results are also recorded in Table 2. For both the CEMs and AEMs, τ_3^D values decreased with increasing IEC, suggesting a decrease in the average size of free volume elements with increasing fixed charge group concentration. Addition of ionizable groups (e.g., sulfonate and quaternary ammonium ions) to a polymer backbone could influence the average size of free volume elements of dry polymers in at least two different ways. First, addition of such moieties could lead to increased attractive interactions between polymer chains due to the polar nature of such functional groups, resulting in more efficient chain packing and subsequent decrease in average size of free volume elements [40]. Alternatively, the bulky nature of the fixed charge groups could disrupt chain packing and thereby increase average free volume element size [40]. The results presented in Fig. 6 suggest that the former effect plays a dominant role in these materials, which agrees with previously published reports on similar materials [40,65].

In general, the CEMs have smaller average free volume elements than the AEMs at all IEC values. However, the CEMs have 30% greater relative concentration (I_3^D) than their AEM counterparts indicating significantly greater density of free volume elements. However, since the presence of electron withdrawing moieties may render I_3^D insensitive to changes in free volume element concentration, limited interpretation of the effects of increased IEC concentration on density of free volume elements can be made.

o-Ps lifetime and intensity values for the hydrated membranes, τ_3^H and I_3^H, respectively, are presented in Fig. 7 and Table 3. For all membranes, τ_3^H values for hydrated samples were greater than those for dry samples, suggesting an increase in average free volume element size upon hydration, presumably due to plasticization of the polymer chains by water and subsequent disruption of interactions between polymer chains. Moreover, τ_3^H values for all membranes were equal to or greater than the τ_3 value for pure water (1.86 ns) [68], which is reasonable since these membranes are relatively highly swollen (water volume fractions > 0.5). Previous reports of τ_3 values for highly swollen sulfonated polysulfone random copolymers agree with the general trends observed in the present study [40]. For the CEMs, τ_3^H values increased by approximately 15–19% upon hydration, whereas τ_3^H values for the AEMs increased by approximately 8–12%. The greater increase in τ_3^H values with hydration for the CEMs could be explained by the greater degree of swelling for the CEMs relative to that for the AEMs (cf. Fig. 2a).

Interestingly, and in contrast to the values for dry membranes, τ_3^H values for all of the hydrated CEMs were essentially the same, within experimental uncertainties, suggesting that the average free volume element sizes for all hydrated CEMs are equivalent. For the AEMs, τ_3^H values for AA238 and AA267 were similar, within experimental uncertainties, while that for AA200 was somewhat larger, suggesting that the average free volume element size for AA200 is larger than that in AA238 and AA267. These results, with the exception of AA200, agree with the equilibrium water content results for these materials, i.e., water volume fraction values for the CEMs, as well as for the AEMs, were essentially the same. This observation is reasonable since free volume in hydrated polymers has been correlated with membrane water content [40].

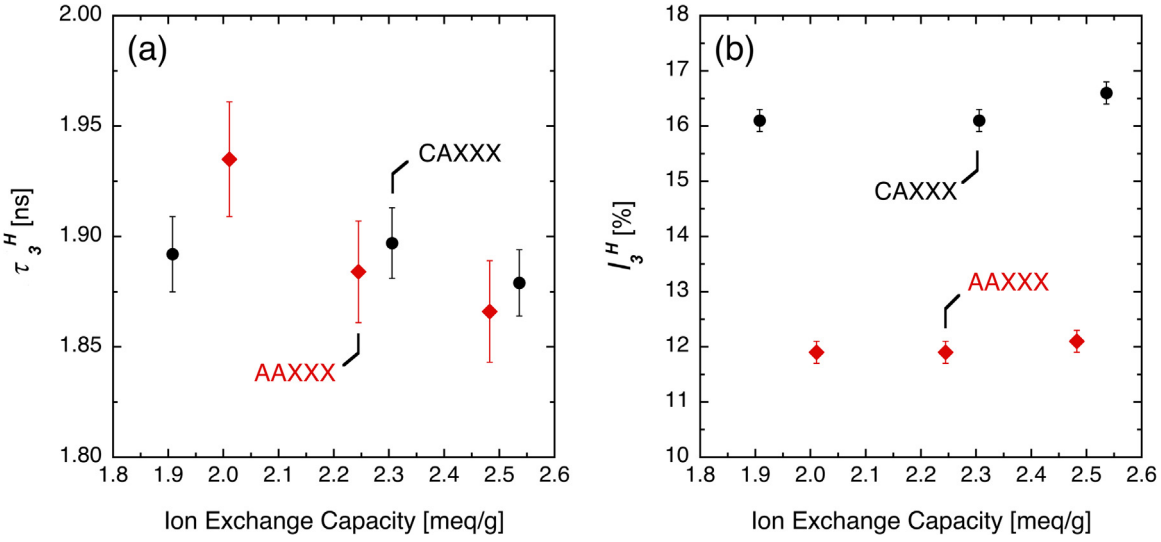

Fig. 7. *o*-Ps lifetime (a) and intensity (b) of hydrated membrane samples as a function of ion exchange capacity. Reported uncertainties are the population standard deviation of measurements on at least 5 sets of data with 1×10^6 integrated counts for each set.

Table 3
PALS results for membranes equilibrated with DI water.

Membrane	τ_3^H [ns]	I_3^H [%]	r^H [nm]	V_{FVE}^H [Å^3]
CA200	1.892 ± 0.017	16.1 ± 0.2	0.550 ± 0.003	87.3 ± 1.6
CA238	1.897 ± 0.016	16.1 ± 0.2	0.551 ± 0.003	87.8 ± 1.5
CA267	1.879 ± 0.015	16.6 ± 0.2	0.548 ± 0.003	86.2 ± 1.4
AA200	1.935 ± 0.026	11.9 ± 0.2	0.559 ± 0.005	91.3 ± 2.4
AA238	1.884 ± 0.023	11.9 ± 0.2	0.549 ± 0.005	86.6 ± 2.1
AA267	1.866 ± 0.023	12.1 ± 0.2	0.545 ± 0.005	85.0 ± 2.1

For the materials considered in this study, and perhaps for other IEMs having similar properties, it appears that the average free volume element size for hydrated samples does not change substantially with changes in fixed charge group concentrations, provided the membrane water content remains constant. Interestingly, a previous study reported that τ_3 values for a series of hydrated sulfonated polysulfone random copolymers correlated well with ion exchange capacity, i.e., τ_3 values increased with increasing IEC, which contrasts with the observations made in the present study [40]. This discrepancy can be explained by considering differences in membrane water content resulting from differences in polymer structure. The IEMs studied by Xie et al. were made from linear polymers, whereas those used in the present study were made from cross-linked polymers [40]. As mentioned earlier, equilibrium water content for membranes made from linear polymers typically increases with increasing IEC due to increased polymer hydrophilicity. In the study by Xie et al., τ_3 values correlated well with membrane water content, regardless of polymer IEC and membrane counter-ion form [40]. These results, as well as those in the present study, support the hypothesis that the average free volume element size in hydrated IEMs correlates more strongly with equilibrium membrane water content than concentration of fixed charge groups.

The *o*-Ps intensities for the hydrated CEMs and AA200 decreased somewhat upon hydration, whereas *o*-Ps intensities for hydrated AA238 and AA267 were more or less similar to values for the dry membranes. However, as mentioned earlier, *o*-Ps inhibition by electron withdrawing moieties can make it difficult to interpret *o*-Ps intensity results, so we do not place much weight on these interpretations. The *o*-Ps intensities for the CEMs, as well as the AEMs, did not change substantially with changes in fixed charge group concentration, suggesting that the density of free volume elements for all CEMs and all AEMs were similar, and the density of free volume elements in the CEMs is greater, on average, than that in the AEMs. These results are in agreement with equilibrium water content values for these materials, i.e., equilibrium water content for the CEMs is greater than that for the AEMs.

To make connections between salt diffusion coefficients and average size of free volume elements, as measured by PALS, average apparent salt diffusion coefficients are presented in Fig. 8 as a function of τ_3 values for the hydrated membranes. Average apparent salt diffusion coefficients represent apparent salt diffusion coefficients averaged over the entire upstream salt concentration range explored in this study. In general, average apparent salt diffusion coefficients correlate well with τ_3, and thus average free volume element size. For the CEMs, average apparent salt diffusion coefficients for CA200 and CA238 were essentially the same, within experimental uncertainties, as were τ_3 values. The average apparent salt diffusion coefficient for CA267 was slightly lower than that for the other two CEMs, and this is explained by the slightly smaller average free volume element size for this material

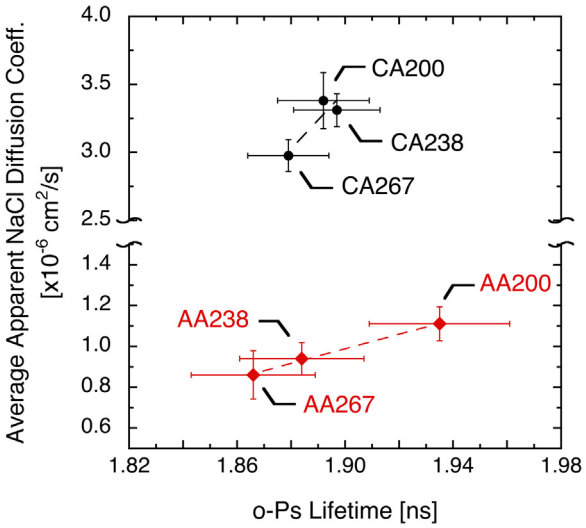

Fig. 8. Average apparent salt diffusion coefficients as a function of τ_3 values. Average apparent salt diffusion coefficients represent apparent salt diffusion coefficients averaged over the entire upstream salt concentration range.

compared to those for the other two CEMs. Average apparent salt diffusion coefficients, as well as τ_3 values, for AA238 and AA267 were similar, within experimental uncertainties, whereas both parameters were slightly larger for AA200.

The results presented in this study further support the hypothesis that equilibrium water content in ion exchange membranes is a good, although not perfect, proxy for average size of free volume elements for such materials. Within experimental uncertainties, water volume fraction values for the CEMs and AEMs were essentially the same. However, slight differences in average membrane free volume element size, as determined via PALS, for CA267 and AA200 compared to the other CEMs and AEMs, respectively, were observed. These differences in average free volume element size adequately explained the small differences in average apparent salt diffusion coefficients for these materials. These results suggest that changes in electrostatic interactions between the fixed charge groups and mobile ions resulting from changes in fixed charge group concentration did not significantly influence salt diffusion coefficients. This conclusion is reasonable since concentration gradient driven ion transport in IEMs is governed by co-ions, and co-ions are likely to diffuse in the aqueous regions of a hydrated IEM, as far away from the fixed charge groups as possible to minimize repulsive electrostatic interactions. For highly swollen membranes, such as those considered here, these interactions are likely to be minimal. It would be of interest to see whether the general trends observed in this study persist for membranes that do not swell as much as the membranes used in the present study. It is reasonable to suppose that specific interactions between polymer chains and mobile ions are likely to be more important for low water content polymers, but such studies remain to be performed.

4. Conclusions

Cation and anion exchange membranes having different fixed charge group concentrations and similar water content were synthesized via free radical copolymerization of a charged monomer and cross-linker in a common solvent. Membrane salt permeability coefficients were measured as a function of upstream NaCl concentration, ranging from 0.01 to 1 M. The salt permeability coefficients were combined with previously reported salt partition coefficients to calculate apparent membrane salt diffusion coefficients via the solution-diffusion model. Apparent salt diffusion coefficients for all membranes were relatively constant over the upstream NaCl concentration range explored in this study and decreased somewhat with increasing membrane fixed charge group concentration. Apparent salt diffusion coefficients for the CEMs decreased to a greater extent than those for the AEMs, despite similar increases in fixed charge group concentration. Modeling results, based on Manning's counter-ion condensation theory, suggested that this observation cannot be explained by electrostatic effects on salt diffusion in these membranes.

Positron annihilation lifetime spectroscopy was employed to quantify the free volume of the IEMs and further explore the influence of polymer structure on ion transport properties. In the dry state, the average free volume element size of the membranes, quantified by τ_3, decreased with increasing fixed charge group concentration, presumably due to enhanced interactions between the polar charged groups that likely resulted in more efficient chain packing. For all membranes, τ_3 values increased upon hydration, indicating plasticization of the polymer chains and subsequent disruption of chain packing. Interestingly, τ_3 values for the hydrated membranes did not depend significantly on IEC, which is likely a consequence of the similar membrane water content of the materials. Average apparent salt diffusion coefficients correlated well with τ_3 values for the hydrated membranes, suggesting that changes in salt diffusion coefficients with increasing fixed charge group concentrations were due to slight variation in membrane free volume, rather than changes in electrostatic interactions between the fixed charge groups and the ions.

Acknowledgements

This material is based upon work supported in part by the National Science Foundation (NSF) Graduate Research Fellowship under Grant No. DGE-1110007, the Welch Foundation Grant No. F-1924-20170325, the Division of Chemical Sciences, Geosciences, and Biosciences (Grant # DE-FG18-02ER15362), Office of Basic Energy Sciences of the U.S. Department of Energy, and by the Australian-American Fulbright Commission for the award to BDF of the U.S. Fulbright Distinguished Chair in Science, Technology and Innovation sponsored by the Commonwealth Scientific and Industrial Research Organization (CSIRO). CMD acknowledges the support of Australian Research Council under award DE140101359 and the Veski Inspiring Women Fellowship.

Appendix A. Supplementary information

Ion diffusion coefficients in ion exchange membranes – electrostatic effects.

Supplementary data associated with this article can be found in the online version at doi:10.1016/j.memsci.2018.08.053.

References

[1] M. Elimelech, W.A. Phillip, The future of seawater desalination: energy, technology, and the environment, Science 333 (2011) 712–717.
[2] M.A. Shannon, P.W. Bohn, M. Elimelech, J.G. Georgiadis, B.J. Marinas, A.M. Mayes, Science and technology for water purification in the coming decades, Nature 452 (2008) 301–310.
[3] N. Ghaffour, T.M. Missimer, G.L. Amy, Technical review and evaluation of the economics of water desalination: current and future challenges for better water supply sustainability, Desalination 309 (2013) 197–207.
[4] H.B. Park, J. Kamcev, L.M. Robeson, M. Elimelech, B.D. Freeman, Maximizing the right stuff: the trade-off between membrane permeability and selectivity, Science 356 (2017).
[5] R.W. Baker, Membrane Technology and Applications, 2nd ed., J. Wiley, Chichester; New York, 2004.
[6] G.M. Geise, H.S. Lee, D.J. Miller, B.D. Freeman, J.E. Mcgrath, D.R. Paul, Water purification by membranes: the role of polymer science, J. Polym. Sci. Polym. Phys. 48 (2010) 1685–1718.
[7] L.F. Greenlee, D.F. Lawler, B.D. Freeman, B. Marrot, P. Moulin, Reverse osmosis desalination: water sources, technology, and today's challenges, Water Res. 43 (2009) 2317–2348.
[8] J.R. Werber, C.O. Osuji, M. Elimelech, Materials for next-generation desalination and water purification membranes, Nat. Rev. Mater. 1 (2016) 1–15.
[9] J. Grimm, D. Bessarabov, R. Sanderson, Review of electro-assisted methods for water purification, Desalination 115 (1998) 285–294.
[10] T.W. Xu, C.H. Huang, Electrodialysis-based separation technologies: a critical review, AIChE J. 54 (2008) 3147–3159.
[11] T.S. Chung, S. Zhang, K.Y. Wang, J.C. Su, M.M. Ling, Forward osmosis processes: yesterday, today and tomorrow, Desalination 287 (2012) 78–81.
[12] D.L. Shaffer, J.R. Werber, H. Jaramillo, S. Lin, M. Elimelech, Forward osmosis: where are we now? Desalination 356 (2015) 271–284.
[13] F.A. AlMarzooqi, A.A. Al Ghaferi, I. Saadat, N. Hilal, Application of capacitive deionisation in water desalination: a review, Desalination 342 (2014) 3–15.
[14] S. Porada, R. Zhao, A. van der Wal, V. Presser, P.M. Biesheuvel, Review on the science and technology of water desalination by capacitive deionization, Prog. Mater. Sci. 58 (2013) 1388–1442.
[15] G.M. Geise, D.R. Paul, B.D. Freeman, Fundamental water and salt transport properties of polymeric materials, Prog. Polym. Sci. 39 (2014) 1–42.
[16] D.R. Paul, Reformulation of the solution-diffusion theory of reverse osmosis, J. Membr. Sci. 241 (2004) 371–386.
[17] J.G. Wijmans, R.W. Baker, The solution-diffusion model: a review, J. Membr. Sci. 107 (1995) 1–21.
[18] J. Ran, L. Wu, Y.B. He, Z.J. Yang, Y.M. Wang, C.X. Jiang, L. Ge, E. Bakangura, T.W. Xu, Ion exchange membranes: new developments and applications, J. Membr. Sci. 522 (2017) 267–291.
[19] M.A. Hickner, Ion-containing polymers: new energy & clean water, Mater. Today 13 (2010) 34–41.
[20] J. Kamcev, B.D. Freeman, Charged polymer membranes for environmental/energy applications, Annu. Rev. Chem. Biomol. Eng. 7 (2016) 111–133.
[21] F. Helfferich, Ion Exchange, Dover Publications, New York, 1995.
[22] J. Kamcev, D.R. Paul, B.D. Freeman, Ion activity coefficients in ion exchange polymers: applicability of manning's counterion condensation theory, Macromolecules 48 (2015) 8011–8024.
[23] J. Kamcev, M. Galizia, F.M. Benedetti, E.S. Jang, D.R. Paul, B.D. Freeman, G.S. Manning, Partitioning of mobile ions between ion exchange polymers and aqueous salt solutions: importance of counter-ion condensation, Phys. Chem. Chem.

Phys. 18 (2016) 6021–6031.
[24] J. Kamcev, D.R. Paul, G.S. Manning, B.D. Freeman, Accounting for frame of reference and thermodynamic non-idealities when calculating salt diffusion coefficients in ion exchange membranes, J. Membr. Sci. 537 (2016) 396–406.
[25] J. Kamcev, D.R. Paul, B.D. Freeman, Effect of fixed charge group concentration on equilibrium ion sorption in ion exchange membranes, J. Mater. Chem. A 5 (2017) 4638–4650.
[26] J. Kamcev, D.R. Paul, G.S. Manning, B.D. Freeman, Predicting salt permeability coefficients in highly swollen, highly charged ion exchange membranes, ACS Appl. Mater. Interfaces 9 (2017) 4044–4056.
[27] G.M. Geise, B.D. Freeman, D.R. Paul, Characterization of a novel sulfonated pentablock copolymer for desalination applications, Polymer 51 (2010) 5815–5822.
[28] G.M. Geise, M.A. Hickner, B.E. Logan, Ionic resistance and permselectivity tradeoffs in anion exchange membranes, ACS Appl. Mater. Interfaces 5 (2013) 10294–10301.
[29] J. Crank, G. Park, Diffusion in Polymers, Academic Press, London, 1968.
[30] N. Lakshminarayanaiah, Transport Phenomena in Membranes, Academic Press, London, 1972.
[31] T. Sata, Ion Exchange Membranes, The Royal Society of Chemistry, Cambridge, 2004.
[32] H. Strathmann, Ion-Exchange Membrane Separation Processes, Elsevier, Amsterdam, 2004.
[33] G.M. Geise, L.P. Falcon, B.D. Freeman, D.R. Paul, Sodium chloride sorption in sulfonated polymers for membrane applications, J. Membr. Sci. 423 (2012) 195–208.
[34] H.B. Park, B.D. Freeman, Z.B. Zhang, M. Sankir, J.E. McGrath, Highly chlorine-tolerant polymers for desalination, Angew. Chem. Int. Ed. 47 (2008) 6019–6024.
[35] X.F. Li, H.M. Zhang, Z.S. Mai, H.Z. Zhang, I. Vankelecom, Ion exchange membranes for vanadium redox flow battery (vrb) applications, Energy Environ. Sci. 4 (2011) 1147–1160.
[36] Y.B. Liu, Z.J. Cai, L. Tan, L. Li, Ion exchange membranes as electrolyte for high performance li-ion batteries, Energy Environ. Sci. 5 (2012) 9007–9013.
[37] T. Mohammadi, M. Skyllas-Kazacos, Characterization of novel composite membrane for redox flow battery applications, J. Membr. Sci. 98 (1995) 77–87.
[38] T. Luo, S. Abdu, M. Wessling, Selectivity of ion exchange membranes: a review, J. Membr. Sci. 555 (2018) 429–454.
[39] M.R. Tant, K.A. Mauritz, G.L. Wilkes, Ionomers: Synthesis, Structure, Properties, and Applications, 1st ed., Blackie Academic & Professional, London; New York, 1997.
[40] W. Xie, J. Cook, H.B. Park, B.D. Freeman, C.H. Lee, J.E. McGrath, Fundamental salt and water transport properties in directly copolymerized disulfonated poly(arylene ether sulfone) random copolymers, Polymer 52 (2011) 2032–2043.
[41] C.S. Gudipati, R.J. MacDonald, Cation Exchange Materials Prepared in Aqueous Media, US Patent 2013/0064982 A1, 2013.
[42] R.J. MacDonald, Synthesis of Highly Cross-Linked Cation-Exchange Polymers from an Aqueous Solution, US Patent 4617321, 1986.
[43] J. Kamcev, E.S. Jang, N. Yan, D.R. Paul, B.D. Freeman, Effect of ambient carbon dioxide on salt permeability and sorption measurements in ion-exchange membranes, J. Membr. Sci. 479 (2015) 55–66.
[44] H. Yasuda, C.E. Lamaze, L.D. Ikenberry, Permeability of solutes through hydrated polymer membranes i. Diffusion of sodium chloride, Makromol. Chem. 118 (1968) 19–35.
[45] W. Stumm, J.J. Morgan, Aquatic Chemistry Chemical Equilibria and Rates in Natural Waters, 3rd ed., Wiley, New York, 1996.
[46] J. Kansy, Microcomputer program for analysis of positron annihilation lifetime spectra, Nucl. Instrum. Methods A 374 (1996) 235–244.
[47] M. Eldrup, D. Lightbody, J.N. Sherwood, The temperature-dependence of positron lifetimes in solid pivalic acid, Chem. Phys. 63 (1981) 51–58.
[48] S.J. Tao, Positronium annihilation in molecular substances, J. Chem. Phys. 56 (1972) 5499–5510.
[49] H. Yasuda, C.E. Lamaze, A. Peterlin, Diffusive and hydraulic permeabilities of water in water-swollen polymer membranes, J. Polym. Sci. A2 (9) (1971) 1117–1131.
[50] H. Ju, A.C. Sagle, B.D. Freeman, J.I. Mardel, A.J. Hill, Characterization of sodium chloride and water transport in crosslinked poly(ethylene oxide) hydrogels, J. Membr. Sci. 358 (2010) 131–141.
[51] A.C. Sagle, H. Ju, B.D. Freeman, M.M. Sharma, Peg-based hydrogel membrane coatings, Polymer 50 (2009) 756–766.
[52] Y.H. Wu, H.B. Park, T. Kai, B.D. Freeman, D.S. Kalika, Water uptake, transport and structure characterization in poly(ethylene glycol) diacrylate hydrogels, J. Membr. Sci. 347 (2010) 197–208.
[53] N.A. Peppas, H.J. Moynihan, L.M. Lucht, The structure of highly crosslinked poly(2-hydroxyethyl methacrylate) hydrogels, J. Biomed. Mater. Res. 19 (1985) 397–411.
[54] G.S. Manning, Limiting laws and counterion condensation in polyelectrolyte solutions. I. Colligative properties, J. Chem. Phys. 51 (1969) 924–933.
[55] J.S. Mackie, P. Meares, The diffusion of electrolytes in a cation-exchange resin membrane. 1. Theoretical, Proc. R. Soc. Lond. Ser.-A 232 (1955) 498–509.
[56] G.S. Manning, Limiting laws and counterion condensation in polyelectrolyte solutions ii. Self-diffusion of the small ions, J. Chem. Phys. 51 (1969) 934–938.
[57] A.J. Hill, B.D. Freeman, M. Jaffe, T.C. Merkel, I. Pinnau, Tailoring nanospace, J. Mol. Struct. 739 (2005) 173–178.
[58] Y.C. Jean, Positron-annihilation spectroscopy for chemical-analysis – a novel probe for microstructural analysis of polymers, Microchem. J. 42 (1990) 72–102.
[59] Y.C. Jean, P.E. Mallon, D.M. Schrader, Principles and Applications of Positron & Positronium Chemistry, World Scientific, Singapore; Hong Kong, 2003.
[60] D.M. Schrader, Y.C. Jean, Positron and Positronium Chemistry, Elsevier, Amsterdam The Netherlands: New York, 1988.
[61] G.Q. Chen, C.A. Scholes, C.M. Doherty, A.J. Hill, G.G. Qiao, S.E. Kentish, Modeling of the sorption and transport properties of water vapor in polyimide membranes, J. Membr. Sci. 409 (2012) 96–104.
[62] H.F.M. Mohamed, Y. Kobayashi, C.S. Kuroda, A. Ohira, Effects of ion exchange on the free volume and oxygen permeation in nafion for fuel cells, J. Phys. Chem. B 113 (2009) 2247–2252.
[63] B.W. Rowe, S.J. Pas, A.J. Hill, R. Suzuki, B.D. Freeman, D.R. Paul, A variable energy positron annihilation lifetime spectroscopy study of physical aging in thin glassy polymer films, Polymer 50 (2009) 6149–6156.
[64] H.H. Yin, Z.J. Yin, W.T. Ma, D.M. Zhu, A review of studies of polymeric membranes by positron annihilation lifetime spectroscopy, Plasma Sci. Technol. 7 (2005) 3062–3064.
[65] G.M. Geise, C.M. Doherty, A.J. Hill, B.D. Freeman, D.R. Paul, Free volume characterization of sulfonated styrenic pentablock copolymers using positron annihilation lifetime spectroscopy, J. Membr. Sci. 453 (2014) 425–434.
[66] Y. Kobayashi, H.F.M. Mohamed, A. Ohira, Positronium formation in aromatic polymer electrolytes for fuel cells, J. Phys. Chem. B 113 (2009) 5698–5701.
[67] K. Hirata, Y. Kobayashi, Y. Ujihira, Effect of halogenated compounds on positronium formation in polycarbonate and polysulfone matrices, J. Chem. Soc. Faraday Trans. 93 (1997) 139–142.
[68] M. Eldrup, O. Mogensen, G. Trumpy, Positron lifetimes in pure and doped ice and in water, J. Chem. Phys. 57 (1972) 495–504.